ELSEVIER

International Journal of Psychophysiology 26 (1997) 63–76

INTERNATIONAL JOURNAL OF PSYCHOPHYSIOLOGY

Study of human occipital alpha rhythm: the alphon hypothesis and alpha suppression

S.J. Williamson, L. Kaufman, Z.-L. Lu, J.-Z. Wang, D. Karron

Neuromagnetism Laboratory, Departments of Physics and Psychology, and Center for Neural Science, New York University, New York, NY 10003, USA

Abstract

Alpha rhythm of the parieto-occipital area is comprised of a parade of short-lived cortical excitations (alphons), each of which exhibits oscillations having a stable period within the alpha bandwidth. Strong alpha rhythm is produced by alphons extending over a larger cortical area, although an enhanced cortical current density may also contribute. Local suppression of alpha rhythm indicates when specific cortical areas become engaged in sensory or cognitive functions. Examples are provided for mental imagery, visual memory, auditory memory, and silent rhythming. © 1997 Elsevier Science B.V.

Keywords: Alpha rhythm; Occipital; Human; Alphon hypothesis; Alpha suppression

1. Introduction

Alpha suppression is no longer considered as a global phenomenon reflecting generalized arousal. Rather, it occurs in specific regions of the cortex, and it depends upon the tasks in which those regions are engaged. Thus, visual stimulation results in modulation of occipital alpha activity, and the modulation envelope fluctuates in-step with the visual stimulus (Kaufman and Locker, 1970). Also, as will be described here, searching memory for previously seen visual forms results in suppression of occipital alpha. Moreover, the duration of this suppression varies with the time required for the subject to indicate completion of the task. In auditory studies, searching short-term memory for previously heard tones results in a similar suppression of alpha. However, in this task the duration of suppression that best correlates with the subject's reaction time occurs over the right temporal cortex. Other cortical sites exhibit alpha suppression too, and these all depend upon the modality involved as well as the nature of the mental task itself. It is now clear that changes in ongoing alpha activity, and possibly in other intrinsic brain rhythms as well, provide a new dimension for the study of brain activity. We are no longer limited to the classic event-related potential which is time-locked to a specific event. We shall give two examples here of spatially selective suppression (desynchronization) of the occipital alpha rhythm, as monitored by neuromagnetic techniques. By having deduced the respective cortical region that produces each rhythm, we may infer that these same regions are involved in the processing that supports the re-

0167-8760/97/$17.00
PII S0167-8760(97)00756-3

spective mental tasks. It is increasingly apparent that the modulation of ongoing brain activity provides a new dimension for the study of cognition (Basar, 1980).

We provide evidence that the occipital alpha rhythm measured within the bandwidth 8–13 Hz can be accounted for by transiently appearing excitations of local cortical regions. These rhythmic excitations — here referred to as 'alphons' — are known to be associated with thalamo–cortical as well as cortico–cortical interactions (Lopes da Silva and van Leeuwen, 1978). The spatio–temporal evolution in these cortical excitations is analogous to a parade of events that produces the changing pattern in the alpha magnetic field outside the head. The conceptual tools we developed to deal with these hypothetical alphons may be extremely useful in mapping the locations at which ongoing activity changes while performing different cognitive tasks. These tools complement a mathematical procedure we have developed for calculating the generalized inverse for field power measurements. This provides a best estimate for the cortical patterns of current power that underlie observed average alpha field power at the scalp. The latter approach deals with average field power, while studies based on the alphon hypothesis deal with field per se. Thus, both approaches may provide useful information regarding the locations of cortical events related to sensory or cognitive processes.

2. Organization of occipital alpha rhythm

Alpha rhythm can be described in a variety of ways, most of which are discussed in the accompanying papers of this volume. Among the most popular are the spectral power and covariance distributions across the scalp. One of the prime aims of our research is to provide a more detailed understanding of its cortical presentation in human subjects, so that we may gain insight for its physiological basis and how it is modulated when the cortex is called upon to carry out sensory or cognitive functions. In particular, this report focuses on the parieto–occipital alpha rhythm as a prototype. We suggest that characteristic features of the time series recorded in measurements of the magnetic field near the occipital scalp provide evidence that the underlying cortical source consists of a parade of excitations at different locations that individually grow and subside in strength. At peak strength, each extends across a cortical area of about 3 cm^2 for human subjects exhibiting a strong alpha rhythm.

3. Nature of alpha rhythm

The physiological basis of occipital alpha rhythm is well established. The initial oscillation is generated within the thalamus by a circuit involving neurons whose membranes exhibit intrinsic oscillatory behavior (Jahnsen and Llinás, 1984a,b; Steriade et al., 1990). Bursts of oscillations are projected onto different cortical locations, from which they spread at a rate (in dog) of 0.3–1 m/s. Consequently, within one period of the oscillation, the cortical excitation could extend a distance of approximately 3 cm. It has been suggested (e.g. Lopes da Silva, 1991) that a function of the alpha rhythm may be to set the mean level of the cortical membrane potential within an extensive local area of cortex.

One of the curiosities of alpha rhythm in the EEG is that its amplitude distribution cannot be distinguished from that of narrow-band filtered Gausssian noise (Dick and Vaughn, 1970). That is, if the time series is sampled at regular time intervals, the number of samples for a given amplitude plotted against amplitude has a normal probability distribution. The Rayleigh probability distribution is characterized by one parameter, so the amplitude and standard deviation of the distribution are related by a multiplicative constant. Whether a time series can be characterized by a normal distribution is easily established by representing the data on a probability, or 'QQ' plot (Becker et al., 1988) and determining whether the trend is described by a straight line. This feature was demonstrated for MEG measurements by Kalimi (1991).

To characterize the key attributes of occipital alpha rhythm, neuromagnetic recordings were made by positioning two cryogenic dewars at the back of the head, one on each side of the midline as illustrated in Fig. 1. Each dewar contains an

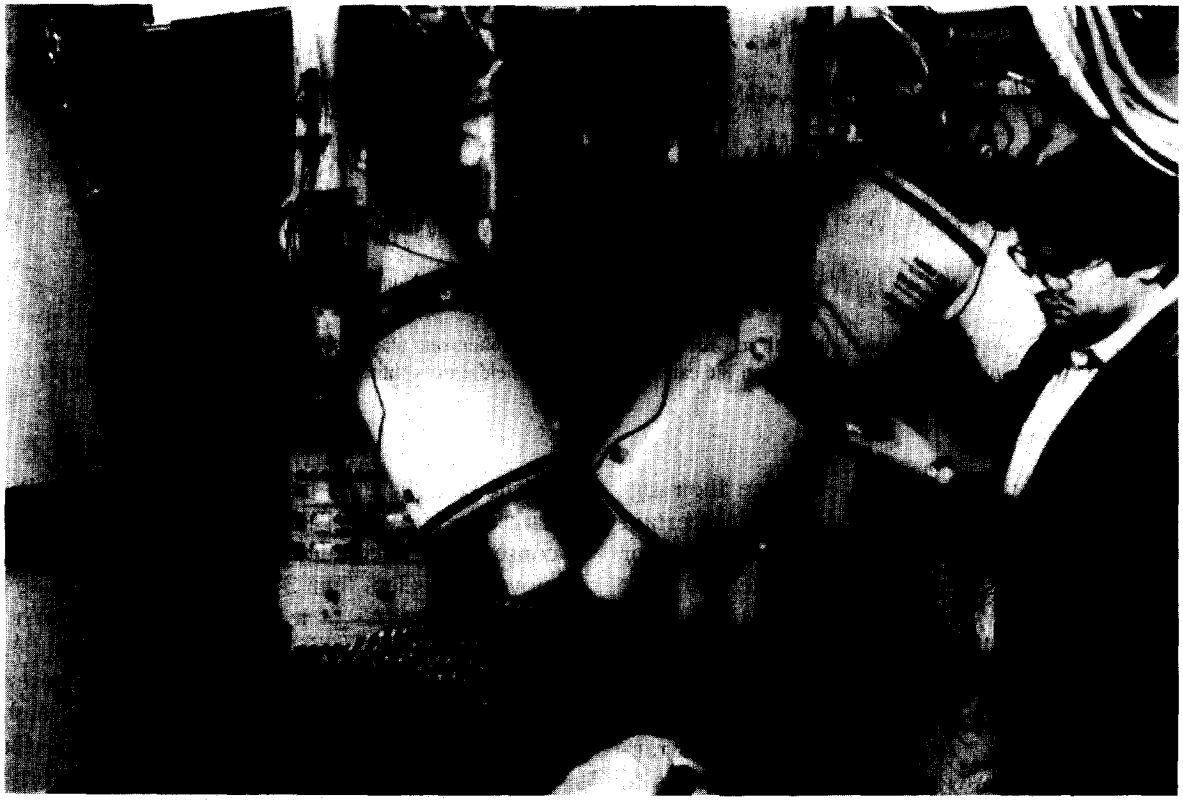

Fig. 1. Arrangement for two sets of superconducting sensors, each within a cryogenic dewar for simultaneously recording magnetic fields of the alpha rhythm over left and right occipital areas of the scalp (Ilmoniemi et al., 1988).

array of seven superconducting sensors to monitor the time sequence, so it is possible to identify coherent signals detected simultaneously over both hemispheres. The characteristic feature of these AC recordings shows the magnetic field emerging from one hemisphere and entering the other, with the locations of strongest field approximately the same distance to the left and right of the midline. This implies that the locations of the sources are near or within the longitudinal fissure. Moreover, the locations where the magnetic field is strongest are nearly opposite each other with respect to the midline, joined by a line that is within 20° of being perpendicular to the midline. We may infer that the underlying intracellular current producing the field is oriented nearly parallel with the longitudinal fissure. Consequently, these sources lie largely within the sulci that extend from the fissure into the left and right hemispheres. Fig. 2 shows a time series of alpha rhythm narrow-band filtered to include only the bandwidth from 8 to 16 Hz.

This illustrates the typical waveform of occipital alpha rhythm, which is commonly described as a series of spindles. There is strong phase coherence throughout the duration of a spindle. If the second harmonic component (within 16–24 Hz) is not removed by filtering, the strongest oscillations may exhibit an arcuate waveform where peaks of one polarity are sharp while peaks of the opposite polarity are flattened — or even display an indentation as in the mu rhythm of the central sulcus (Tiihonen et al., 1989). The arcuate feature has been clearly recorded with an array of electrodes inserted into the depth of occipital cortex of dog where the polarity of the sharper peak corresponds to intracellular current flowing toward the depth of cortex (Lopes da Silva and van Leeuwen, 1978).

Time series of the alpha rhythm have been

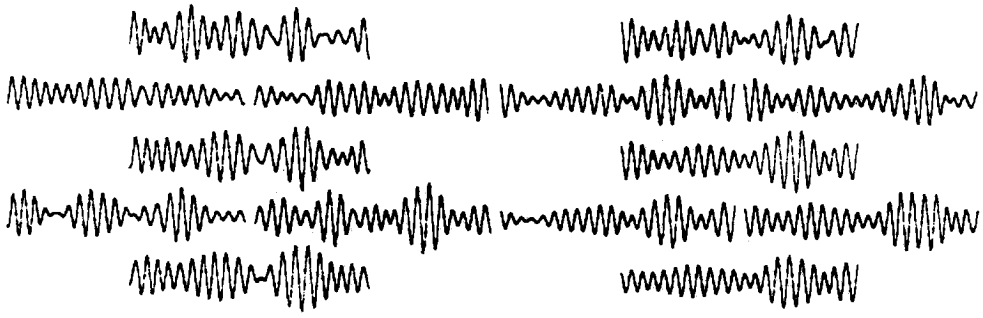

Fig. 2. Time series within the alpha bandwidth recorded by two 7-sensor probes, one placed over the left hemisphere and the other over the right hemisphere. Downward deflection indicates the magnetic field enters the head; upward deflection, it emerges from the head.

analyzed in various ways to determine their significant properties, particularly to ascertain whether they exhibit features of deterministic or random processes (Pritchard and Duke, 1997).

Our analyses of the alpha rhythm time series suggest that the period stability between zero crossings in the waveform (Carelli et al., 1983; Vvedensky et al., 1985) is a key piece of evidence that distinguishes alpha rhythms from pure random noise. One way to analyze these data is to determine how likely it is to have a series of zero-crossings producing a given number of periods exhibiting stability that is greater than a specified level. This exercise has been carried out on our data for the parieto–occipital alpha rhythm obtained on two subjects. The results are sufficient to provide a definitive answer. Table 1 shows that occipital alpha rhythm has a much enhanced period stability over a short time interval than narrow-band filtered noise, even though they have the same amplitude distribution. This suggests that individual alpha sources of these spindles have a temporally coherent structure.

A second aspect that appears in the alpha data is the stability of the magnetic field pattern across individual peaks within a spindle. One way to characterize this is to represent the location of neural activity for each peak by a current dipole. Even if the active cortical area might be much more extensive than is warranted by this model, the dipole approach still provides a useful measure for the spatial stability of the center of the neural excitation. Table 2 illustrates our results by showing the PPN headframe coordinates (Williamson et al., 1991) for the dipole positions of consecutive oscillation peaks. In general, the movement is less than 3 mm during the time span when the periods of a spindle are stable. When one spindle disappears and another appears there is an abrupt change in both location and period. These features indicate that occipital alpha rhythm consists of a parade of excitations that arise in different locations of the cerebral cortex, each excitation exhibiting a fixed period for its oscillations. These characteristics motivated us to introduce the term 'alphon' as a generic term for these cortical excitations (Williamson et al., 1989).

In our study of three subjects, the criteria for identifying alphons within the complicated sequence of spindles was conservative in order to avoid time-series where two or more alphons are superimposed. The peak field must exceed 400 fT for about 300 ms at the mid-point of the oscilla-

Table 1
Number of periods that are stable to within the indicated percentage for gaussian noise within the bandwidth of 8–13 Hz and for alpha rhythm within the same bandwidth for each of three subjects

Condition	1%	3%	5%	10%	30%	50%
Noise recording	15	447	1337	3966	7839	8316
Alpha recording (SW)	1100	2246	4794	6063	7999	8221
Alpha recording (JH)	2828	5294	6125	6904	7763	8109
Alpha recording (ZL)	2136	3891	4506	5228	6384	8171

For both conditions (noise and alpha recordings), the total number of periods considered is 8318.

Table 2
Cartesian coordinates in the PPN headframe indicating the location of the center of activation (X,Y,Z) for the extensive source model that best accounts for the field pattern at successive peaks in three bursts

X (cm)	Y (cm)	Z (cm)	Q(nA m)	*Corr*	χ^2	*P*
−5.69	0.55	6.77	43.7	0.997	0.53	0.86
−5.52	0.19	6.93	53.3	0.997	0.73	0.69
−5.54	0.10	6.81	58.8	0.996	0.97	0.47
−5.40	0.08	6.67	61.8	0.996	0.86	0.56
−5.26	0.15	6.61	56.3	0.996	0.53	0.86
−5.21	0.05	6.48	57.6	0.996	0.54	0.85
−5.31	−0.08	6.89	48.1	0.998	0.31	0.97
−5.29	−0.32	6.04	72.4	0.997	0.62	0.78
−5.10	−0.22	6.42	77.0	0.995	0.90	0.52
−4.94	−0.19	6.64	78.5	0.994	0.99	0.45
−4.92	−0.32	6.82	71.1	0.991	1.02	0.43
−4.82	−0.48	6.58	70.9	0.984	1.00	0.48
−5.63	0.16	6.18	50.0	0.987	1.39	0.19
−5.87	−0.13	6.34	59.8	0.994	1.07	0.38
−5.56	−0.30	6.22	76.7	0.998	0.53	0.86
−5.30	−0.28	6.28	83.5	0.997	0.73	0.68

Notes: Q, total current dipole moment; *Corr*, correlation between the field data and field pattern of the best-fitting model source; χ^2, value of chi square for the best fit; P, gives the probability that chi square is greater or equal to the attained value.

tion sequence, the mean amplitude over the sequence must exceed 150 fT, and the period stability must be better than 5%. With these conditions the period and location of neural activity of an alphon are stable for about six oscillations. The spatial correlations between signals in the array of 14 magnetic field sensors all exceed 0.9 as registered at successive peaks. For this study, alphons exhibiting the strongest magnetic field lie within about 2 cm of the midline. This feature, together with the fact that their current dipole moments lie nearly parallel to the longitudinal fissure, support the notion that these alphons lie within the walls of the sulci that extend into the left and right hemispheres from the longitudinal fissure (Fig. 3).

The strengths of the current–dipole moments deduced from the single current–dipole model are much greater than the strength of long-latency components (100–300 ms) of typical sensory-evoked responses. A representative value of Q = 60 nA·m is considerably stronger than the value of 10 nA·m that is characteristic of a sensory related component. Can this enhancement be due primarily to a greater trans–cortical current? To assess this possibility, we fit the magnetic field data for individual alphons by a finite-area model consisting of nine current dipoles in a 3 × 3 square array, with all the dipoles oriented perpendicular to the surface of the square. The corresponding cortical locations for alphons exhibiting magnetic fields of average strength are substantially more shallow than those obtained from a single current–dipole model, as illustrated in Fig. 4. The reason for this discrepancy is simple. A finite-area model is represented by a field pattern whose locations of maximum inward and outward field are separated by a greater distance than for a current dipole at the same depth. To reproduce a similar separation with a current dipole requires that it be placed deeper beneath the scalp. To emphasize this feature, we note that the alphons in Fig. 3 appearing to be located near or within the cerebellum for the current dipole model are pulled up into the cerebral cortex in the finite-area model as displayed in Fig. 4.

The finite-area model when fitted to our data provides an estimate for the spatial extent of the active cortical area for individual alphons. For our three subjects we obtained the following results based on the typical values for the sum of the moments of all the nine component dipoles in the model: Subject JCH has a total dipole moment of Q = 39 nA·m and an active cortical area of 2.9 cm^2; SJW with Q = 41 nA·m has an area of 2.7 cm^2; and ZL with Q = 35 nA·m has an area of 2.8 cm^2. The values for the active area are remarkably consistent across these three subjects who exhibit strong alpha rhythm. However, the close numerical agreement is no doubt fortuitous, since the finite-area model is certainly too simplistic to provide such accurate values.

Nevertheless, there is a systematic discrepancy between the current-dipole moments obtained with the single current–dipole model and the total current–dipole moments of the finite-area model: the former are typically Q = 60 nA·m, while the later are typically Q = 40 nA·m. Since the estimated active area of 3 cm^2 corresponds to

Fig. 3. Alphon locations deduced from a single current–dipole model, with the background depicting features of the mesial surface of the subject's left hemisphere. for subject SJW. Axes denote the PPN headframe coordinates, with $Y = -0.1$ cm for the MRI slice depicted. Symbols indicate the strengths of the magnetic field extrema: Circle, strongest; triangle, average; square, weakest.

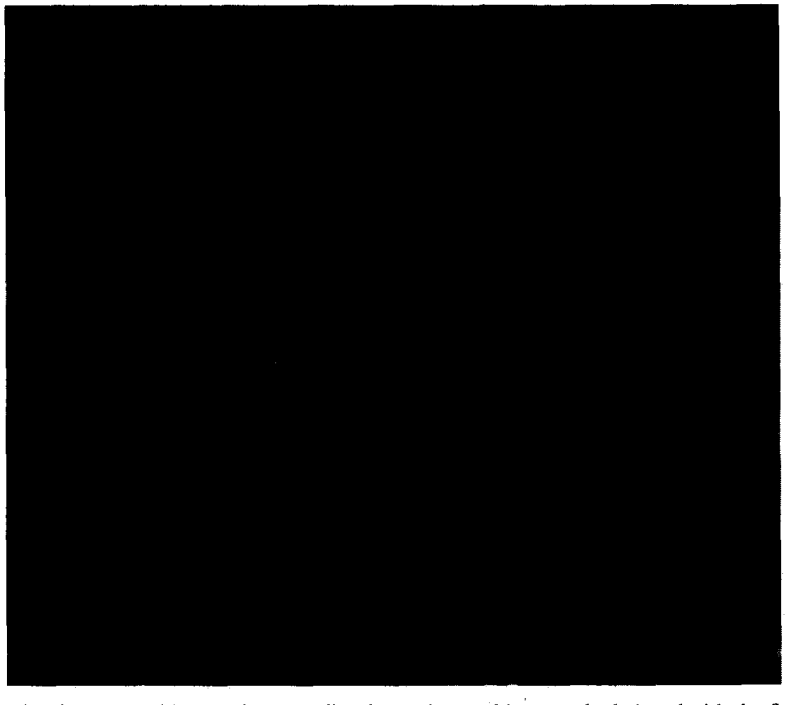

Fig. 4. Alphon locations for the same subject as the preceding figure, but in this example deduced with the finite area model. Shown here are representative cortical excitations of average or greater strength in the left hemisphere.

a characteristic length of about 1.5–2 cm, neglecting the finite extent of an alphon when it lies 3–5 cm beneath the sensors becomes a questionable procedure. Clearly, a comparison of the deduced locations for alphons based on the single-dipole model (Fig. 3) and the finite-area model (Fig. 4) for sources producing representative field strengths shows a marked difference in locations. Consequently, the single-dipole model must be considered inadequate for these sets of data.

From the total current–dipole moment and the active cortical area provided by the finite-area model, we can deduce the current–dipole moment density for this region of cortex. Taking representative values of 40 nA·m and 3 cm^2 respectively, we obtain the value of 130 pA·m/mm^2 for alpha rhythm. This is greater than the value of 50 pA·m/mm^2 obtained from an analysis of current source-density data reported in the literature for long latency sensory evoked components in cat and monkey (Lu and Williamson, 1991). However, the uncertainty in the latter value is about a factor of two, because of variability in the measurements and re-scaling from animal to human cortex. Therefore, the fact that the magnetic field of a strong alpha rhythm can be more than a factor of five greater than the field of long-latency components of sensory evoked responses is largely due to a greater cortical area of coherent activity, although enhanced cortical current density may also contribute.

4. Alpha suppression

It is well known that the strength of alpha rhythm can be modulated when the supporting cortex becomes engaged in a sensory or cognitive task (Slatter, 1960; Kaufman and Locker, 1970; Pfurtscheller and Aranibar, 1977; Basar, 1980; Klimesch et al., 1988; Pfurtscheller and Klimesch, 1992; Salmelin and Hari, 1994; Hari et al., 1995). One interpretation of alpha suppression is that it reflects the disturbance of an ongoing parade of alphons. Of course there are other possible interpretations. For example, the relative intensity of activity on opposing walls of a sulcus may change, and that will alter the partial cancellation of their superimposed magnetic fields and electric potentials. For instance, if currents are synchronous and oppositely directed, the summated field and potential patterns thus result in a net decrease of alpha power. However, this is an unlikely event, and so it is more instructive to consider a simpler situation in which geometrical effects of the underlying cortical geometry are ignored. In view of the widespread assumption that synchronization underlies alpha enhancement, and desynchronization its blockage, it is instructive to consider possible effects of cortical geometry. Where there is a degree of mirror symmetry in activity, e.g. as when opposed walls of a sulcus are simultaneously active, it is possible to measure a weaker field pattern in the presence of stronger transcortical currents (Kaufman et al., 1992). However, while we must be circumspect in attributing alpha blockage to desynchronization, as opposed to a reduction in level of activity, it is still useful to ignore effects of cortical geometry.

Alpha suppression studies could provide the most meaningful spatial information about locations of sensory or cognitive processes if the spatial extent of an alphon were smaller than the cortical area that serves the specific function of interest. Then an empirical characterization of the change in the statistical aspects of when and where alphons appear could provide more detailed information on aspects of the functional organization within that cortical area. However, lacking that information, we are limited to a simpler class of studies in which deviations from the average properties of alpha rhythm — such as alpha power or variance — are characterized. As illustrations, we shall give two examples of spatially selective suppression of the occipital alpha rhythm as revealed by neuromagnetic techniques. By identifying the cortical region that produces the rhythm that is suppressed, we may infer that this same region is involved in the processing that supports the mental tasks.

4.1. Mental imagery

The first example of alpha suppression recorded neuromagnetically is an application by Kaufman et al. (1990) of the Sternberg paradigm (Sternberg, 1966, 1975) in which a subject is shown a

series of illustrations of abstract figures that are to be remembered. Then a test item is displayed, indicating that the subject must press one button to declare it was a member of the memory set or another button if it is not. The variance about the mean response in the alpha band was recorded to eliminate contributions of Fourier components in the alpha bandwidth from stimulus-locked signals. This gives a measure of alpha power that is totally independent of the event related response (Kaufman and Price, 1967). When each of the figures of the memory set are shown, occipital alpha is briefly suppressed; but when the test figure is shown, the duration of suppression is prolonged. Fig. 5 shows the suppression for both real-time recordings and the variance across a set of recordings.

Neuromagnetic measurements show that the subsequent spatial pattern of alpha suppression is similar to the pattern of suppression for the visual presentation of each of the individual memory items. This finding is evidence that similar neural populations are called into play, thus suggesting that visual cortex participates in the task of mental imagery (Kaufman et al., 1990). This finding is consistent with a recent PET study (Kosslyn et al., 1993) that reported increased activity in Area 17 of visual cortex during mental imagery. Exploiting the rapid response afforded by magnetic measurements, Kaufman et al. (1990) found that the duration of suppression increases with the number of items that comprised the memory set, as was true also for the reaction time first observed by Cooper and Shepard (1973) when using this paradigm in psychophysical studies.

An auditory version of the Sternberg paradigm was also carried out by Kaufman et al. (1992) using neuromagnetic techniques for a memory set of tones having different pitch. When the variance within the alpha band was obtained over the anterior temporal area, where a magnetic field from primary auditory cortex would be expected,

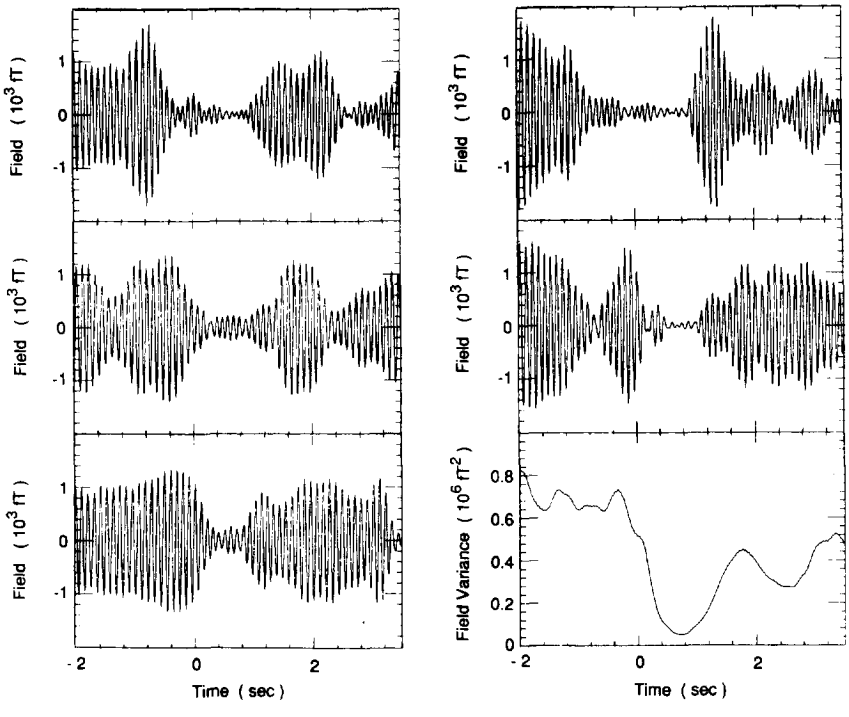

Fig. 5. Time course of alpha suppression after an abstract figure is shown and the subject must determine whether it was a member of a memory set of items previously seen. Five traces show successive real-time recordings, and the lower right trace shows the time course of the low-pass filtered variance averaged across trials.

the duration of alpha suppression increased linearly with the number of tones in the memory set. This was a significant effect over the right hemisphere but not over the left; and the duration of suppression best correlating with the subject's reaction time was that of the left hemisphere. These results supported the notion that the corresponding neural sources could be located within the auditory cortex, a feature that is consistent with the neuromagnetic evidence of Tiihonen et al. (1991) that an alpha rhythm is generated by the supratemporal cortex.

4.2. Visual imagery and silent rhyming

It is of some interest to compare cognitive tasks across modalities, for in this way subtle differences in brain strategies may be revealed. This prospect motivated a study in which the subject viewed a computer monitor and responded to a word that was briefly presented. The overall illumination was kept low, and the peripheral view was featureless so that the subject exhibited strong occipital alpha rhythm with eyes open. In separate studies, alpha power was monitored over the occipital area and left frontal area. In one series of recordings, the subject's task was to watch the computer screen, and when a word is briefly presented to silently find a word that rhymes with the displayed word. In a second series, the subject's task was to find an image of the object that the word represents. Fig. 6 shows the time dependence of the variance within the alpha band in the silent rhyming task. There was but a brief suppression over the occipital area, corresponding to the duration for which visual cortex is expected to participate in processing the visual information. However, after a delay of about 100 ms following the presentation, the onset of alpha power suppression was observed in the left frontal area. This was sustained for at least 1 s, until about the time the subject pressed a reaction

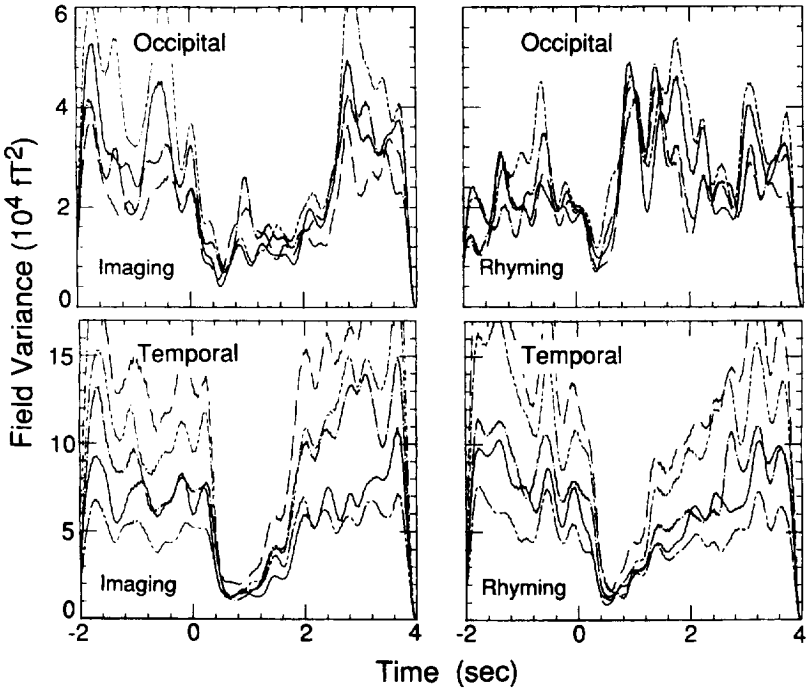

Fig. 6. Variation in the short-term average of alpha power measured with an array of five magnetic field sensors placed over the occipital scalp (upper panels) and left anterior temporal scalp (lower panels) when a subject is engaged in a mental imaging task (left panels) or silent rhyming task (right panels).

time button to indicate he had found a word that rhymes with the one that had been displayed.

In a second series of recordings for the mental imagery task, the subject is instructed to form a mental image of the object that the displayed word represents. Here the alpha variance over the occipital area remained suppressed following the initial response of the visual cortex, until about the time when the subject pressed the reaction time button indicating he had formed a mental image that the word represented. However, a few hundred milliseconds after the onset of the word's display, the temporal area also revealed the onset of suppression, and this was sustained for many hundreds of milliseconds. We can only speculate that perhaps the subject was engaged in 'speaking to himself' when seeking an image that corresponds to the word that had been displayed. Some of the subjects in the present study admitted that they would occasionally speak silently to themselves for words that posed a particularly difficult challenge in finding an image.

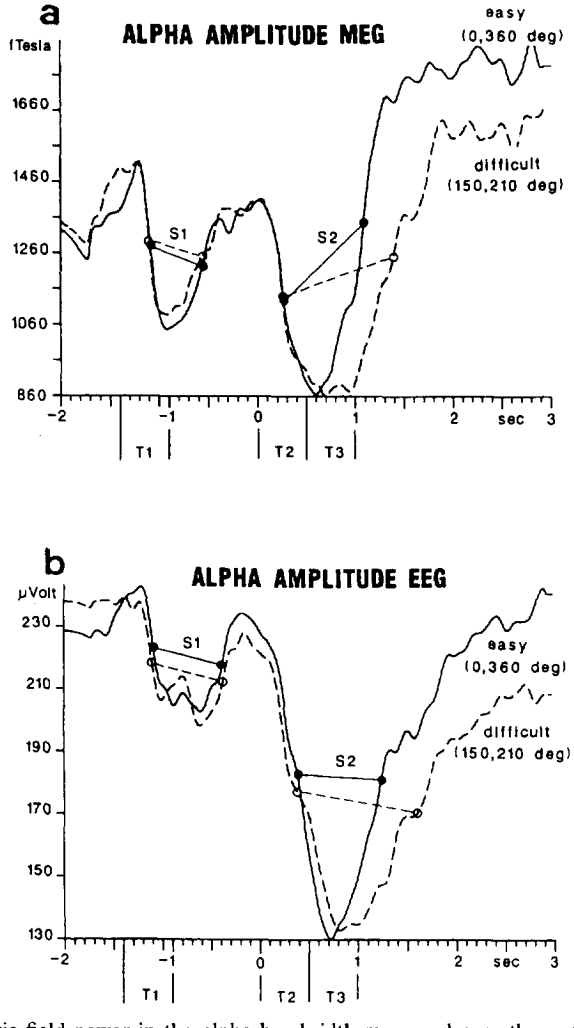

Fig. 7. (a) Suppression of magnetic field power in the alpha bandwidth measured over the occipital scalp after the onset of the presentation of a memory figure *S1* and the test figure *S2* in a mental rotation task. The shift of the broken curve relative to the solid curve illustrates the increase in duration of alpha suppression when the test figure is presented with a large rotation angle with respect to the memory figure (difficult condition). (b) Simultaneous recording of electric potential variance.

Others claimed that they did not. However, other authors have obtained evidence in neuromagnetic studies that a picture shown to a subject who is instructed to remain passive, nevertheless, produces responses within several naming-related brain areas, suggesting that humans may automatically label objects in the environment. These serendipitous findings suggest the prospect whereby continued development in sophistication of alpha suppression techniques may well provide an opportunity to follow the evolution of a subject's thought processes when attempting to overcome difficult challenges.

4.3. Mental rotation

A final example of exploiting the alpha suppression paradigm to identify cortical areas that participate in cognitive functions is provided by a mental rotation task. In this study, each of six subjects was first shown a line drawing of an abstract object, and then after about 1 s another presentation of a test figure that may be the same object rotated or a line drawing of a different object. The subject's task is to press one reaction time button if it is judged to be the same object or a second button if it is not. The classic finding that reaction time increases linearly with rotation angle (Cooper and Shepard, 1973) was reproduced. Moreover, as shown in Fig. 7 Michel et al. (1994) observed a similar increase in duration of alpha suppression with rotation angle. This provides further evidence that visual cortex remains engaged in the cognitive task during the course of manipulating the image to determine whether a match can be made. Of particular interest, when the task is made more difficult by having the test figure rotated by a large angle, the center of the power pattern shifts slightly toward the right parietal area during the later portion of the suppression duration. This may suggest additional suppression of alpha activity in the left occipital area as the brain calls on more neural resources for completion of the task.

5. Perspective

One intepretation of alpha suppression related to an ongoing cognitive process is that it reflects the disturbance in an ongoing parade of alphons. Of course, we are aware of other possible interpretations. For example, the amounts of activity on adjacent walls of cortical sulcus may change to increase or decrease the balance of activity. In some cases this may result in a net increase in cortical current, but a diminished external field (Kaufman et al., 1992). However, it is instructive to consider a simpler situation in which effects of underlying cortical geometry are ignored, and we consider instead how well disturbances in parades of alphons might affect observed alpha rhythms. With the recent development of large arrays of magnetic field sensors that can characterize the spatio–temporal pattern of magnetic field over the entire scalp, it becomes feasible to apply the mathematics of generalized inverse solutions to measurements of both magnetic field (Wang et al., 1992) and magnetic field power (Wang et al., 1993). From the spatial distribution of averaged field power, it is then possible to obtain a magnetic source image (MSI) of the cortical distribution of average current power. In this way, the distribution of cortical activity can be inferred without having to impose a simplified model such as a distribution of a small number of current dipoles. This provides a best estimate for the spatio–temporal distribution of the suppressed cortical activity by subtracting the corresponding MSI defined across the cerebral cortex for field power in the suppressed condition from the MSI in the baseline condition.

A simple illustration of this procedure is given in Fig. 8 for a representation of a small portion of the cerebral cortex. Spontaneous cortical activity is represented by an array of current elements in panel (a), with each element fluctuating independently from the others, with the same mean power level. However, a crescent-shaped region on the left wall has suppressed activity. To compute the inverse solution that will reveal this region of suppression, the baseline distribution of mean magnetic field variance is first recorded for the array of magnetic sensors positioned above this cortical region. Then the spatial pattern of mean variance is recorded during the suppression condition. The inverse solution is determined for

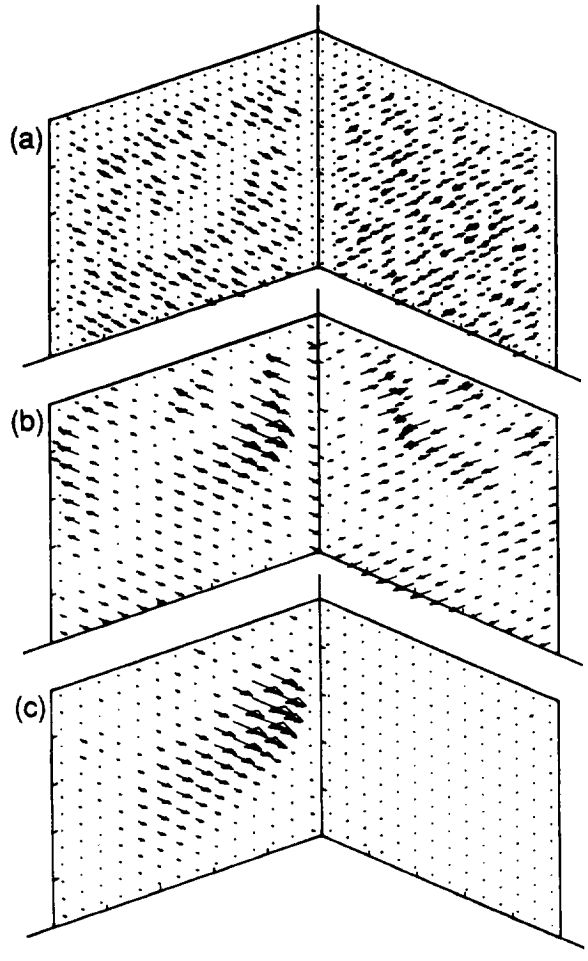

Fig. 8. (a) Snapshot of simulated spontaneous cortical activity represented by short current elements (arrows) distributed across a sulcal wall making a right angle bend. A crescent-shaped patch on the left wall is suppressed. (b) MNLS inverse solution deduced from field power measurements, where the baseline distribution of power does not adequately match the actual distribution that pertained to the measurement. (c) MNLS inverse solution deduced for a proper baseline distribution of power.

each condition, and a best estimate for the cortical locations of suppressed alpha rhythm is obtained by subtracting the image for the suppression condition from the initial baseline image. The corresponding result in Fig. 8 is shown for two cases: the image in panel (b) is obtained when the baseline is improperly estimated, perhaps representing inappropriate averaging or a change in the brain's state during the measurements. The image in panel (c) shows the results when the subtraction is carried out for a proper baseline representation. To achieve these different conditions in the simulations, the same seed was used for starting the computer generation of noise for baseline and suppression conditions in panel (c); whereas, different seeds were employed for panel (b).

By exploiting magnetic source images such as these, it may be possible to characterize the detailed evolution of cortical activity throughout the period when a subject is engaged in a cognitive task. This would provide a dynamical image that quantitatively characterizes how spontaneous cortical rhythms are modulated in space and time across the cerebral cortex. However, the spatial resolution provided by such an image may well be

limited by the coherence length of what we suggest to be the fundamental building block of the alpha rhythm — the alphon.

Acknowledgements

This work was supported in part by a grant to New York University from the Horace W. Goldsmith Foundation.

References

Basar, E. (1980) EEG-brain dynamics: relation between EEG and brain evoked potentials. Elsevier, Amsterdam, North Holland.

Becker, R.A., Chambers, J.M. and Wilks, A.R. (1988) The new S language. A programming environment for data analysis and graphs. Wadsworth and Brooks/Cole, Pacific Grove, CA.

Carelli, P., Foglietti, V., Modena, I. and Romani, G.-L. (1983) Magnetic study of the spontaneous brain activity of normal subjects. Il Nuovo Cimento 2D: 538–546.

Cooper, L.A. and Shepard, R.N. (1973) The time required to prepare for a rotated stimulus. Mem. Cognit., 1: 246–250.

Dick, D.E. and Vaughn, A.O. (1970) Mathematical description and computer detection of alpha waves. Math. Biosci., 7: 81–95.

Hari, R., Salmelin, K., Mäkelä, J.P., Salenius, S. and Helle, M. (1995) Characterization of magnetoencephalographic 10- and 20-Hz rhythms. 26: 51–62.

Ilmoniemi, R.J., Williamson, S.J. and Hostetler, W.E. (1988) New method for the study of spontaneous brain activity. In: K. Atsumi, M. Kotani, S. Ueno, T. Katila and S.J. Williamson (Eds.), Biomagnetism '87, Tokyo Denki University Press, Tokyo, pp. 182–185.

Jahnsen, H. and Llinás, R. (1984a) Electrophysiological properites of guinea-pig thalamic neurones: an in vitro study. J. Physiol. (London), 349: 205–226.

Jahnsen, H. and Llinás, R. (1984b) Ionic basis for the electroresponsiveness and oscillatory properties of guinea-pig thalamic neurones in vitro. J. Physiol. (London), 349: 227–247.

Kalimi, R. (1991) Statistical properties of human alpha rhythm. B.A. Thesis, New York University, New York.

Kaufman, L. and Locker, Y. (1970) Sensory modulation of the EEG. Proc. Am. Psychol. Assoc., 179–180.

Kaufman, L. andPrice, R. (1967) The detection of cortical spike activity at the human scalp. IEEE Trans. Biomed. Eng. BME, 14: 84–90.

Kaufman, L., Schwartz, B., Salustri, C. and Williamson, S.J. (1990) Modulation of spontaneous brain activity during mental imagery. J. Cogn. Neurosci., 2: 124–132.

Kaufman, L., Curtis, S., Wang, J.-Z. and Williamson, S.J. (1992) Changes in cortical activity when subjects scan memory for tones. In: M. Hoke, S.N. Erné, Y.C. Okada, G.-L. Romani (Eds.), Biomagnetism: Clinical Aspects, Excerpta Medica, Elsevier, Amsterdam, pp. 189–193.

Klimesch, W., Pfurtscheller, G. and Mohl, W. (1988) Mapping and long-term memory: The temporal and topographical pattern of cortical activation. In: G. Pfurtscheller and F.H. Lopes Da Silva (Eds.), Functional Brain Imaging, Hans Huber Publishers, Toronto, pp. 131–142.

Kosslyn, S.M., Alpert, N.M., Thompson, W.L., Maljkovic, V., Weise, S.B., Chabris, C.F., Hamilton, S.E., Rauch, S.L. and Buonanno, F.S. (1993) Visual mental imagery activates topographically organized visual cortex: PET investigations. J. Cogn. Neurosci., 5: 263–287.

Lopes da Silva, F.H. (1991) Neural mechanisms underlying brain waves: from neural membranes to networks. Electroencephalogr. Clin. Neurophysiol., 79: 81–93.

Lopes da Silva, F.H. and Storm van Leeuwen, W. (1978) The cortical alpha rhythm in dog: the depth and surface profile of phase. In: M.A.B. Brazier and H. Petsche (Eds.), Architectonics of the Cerebral Cortex, Raven Press, New York, pp. 319–333.

Lu, Z.L. and Williamson, S.J. (1991) Spatial extent of coherent sensory-evoked cortical activity. Exp. Brain Res., 84: 411–416.

Michel, C.M., Kaufman, L. and Williamson, S.J. (1994) Duration of EEG and MEG α suppression increases with angle in a mental rotation task. J. Cogn. Neurosci., 6: 139–149.

Pfurtscheller, G. and Aranibar, A. (1977) Event-related cortical desynchronization detected by power measurments of scalp EEG. Electroenecephalogr. Clin. Neurophysiol., 42: 817–826.

Pfurtscheller, G. and Klimesch, W. (1992) Functional topography during a visuoverbal judgement task studied with event-related desynchronization mapping. J. Clin. Neurophysiol., 9: 120–131.

Pritchard, W.S. and Duke, D.W. (1997) Segregation of the thalamic alpha rhythm from cortical alpha activity using the Savit-Green S statistic and estimated correlation dimension. Int. J. Psychophysiol., 26: 263–271.

Salmelin, R. and Hari, R. (1994) Characterization of spontaneous MEG rhythms in healthy adults. Electroencephalogr. Clin. Neurophysiol., 91: 237–248.

Slatter, K.H. (1960) Alpha rhythm and mental imagery. Electroencephalogr. Clin. Neurophysiol., 12: 851–895.

Steriade, M., Gloor, P., Llinás, R.R., Lopes da Silva, F.H. and Mesulam, M.-M. (1990) Basic mechanisms of cerebral rhythmic activities. Electroencephalogr. Clin. Neurophysiol., 76: 481–508.

Sternberg, S. (1966) High-speed scanning in human memory. Science, 153: 652–654.

Sternberg, S. (1975) Memory scanning: new findings and current controversies. Q. J. Exp. Psychol., 27: 1–32.

Tiihonen, J., Kajola, M. and Hari, R. (1989) Magnetic mu rhythm in man. Neuroscience, 32: 793–800.

Tiihonen, J., Hari, R., Kajola, M., Karhu, J., Ahlfors, S. and Tissari, S. (1991) Magnetoencephalographic 10-Hz rhythm from the human auditory cortex. Neurosci. Lett., 303–305.

Vvedensky, V.L., Naurzakov, S.P., Ozhogin, V.I. and Shabanov, S.Yu. (1985) Measurement of the tangential component of the magnetic field associated with rhythmic alpha activity in the human brain. In: H. Weinberg, G. Stroink, T. Katila (Eds.), Fifth World Conference on Biomagnetism, Pergamon Press, New York, pp. 57–60.

Wang, J.-Z., Williamson, S.W. and Kaufman, L. (1992) Magnetic source images determined by a lead-field analysis: the unique minimum-norm least-squares estimation. IEEE Trans. Biomed. Eng., 39: 665–675.

Wang, J.Z., Kaufman, L. and Williamson, S.J. (1993) Imaging regional changes in the spontaneous activity of the brain: an extension of the minimum norm least-squares estimate. Electroencephalogr. Clin. Neurophysiol., 86: 36–50.

Williamson, S.J., Wang, J.Z. and Ilmoniemi, R.J. (1989) Method for locating sources of human alpha activity. In: S.J. Williamson, M. Hoke, G. Stroink and M. Kotani (Eds.), Advances in Biomagnetism, Plenum, New York, pp. 257–260.

Williamson, S.J., Lu, Z.L., Karron, D. and Kaufman, L. (1991) Advantages and limitations of magnetic source imaging. Brain Topogr., 4: 169–180.